

Gluon–gluon antenna functions from Higgs boson decay

Journal Article**Author(s):**

Gehrmann-De Ridder, Aude; Gehrmann, Thomas; Glover, E.W. Nigel

Publication date:

2005-04-14

Permanent link:

<https://doi.org/10.3929/ethz-b-000033177>

Rights / license:

[Creative Commons Attribution 3.0 Unported](#)

Originally published in:

Physics Letters B 612(1-2), <https://doi.org/10.1016/j.physletb.2005.03.003>



ELSEVIER

Available online at www.sciencedirect.com

SCIENCE @ DIRECT®

Physics Letters B 612 (2005) 49–60

PHYSICS LETTERS B

www.elsevier.com/locate/physletb

Gluon–gluon antenna functions from Higgs boson decay

A. Gehrmann-De Ridder^a, T. Gehrmann^b, E.W.N. Glover^c

^a *Institute for Theoretical Physics, ETH, CH-8093 Zürich, Switzerland*

^b *Institut für Theoretische Physik, Universität Zürich, Winterthurerstrasse 190, CH-8057 Zürich, Switzerland*

^c *Institute for Particle Physics Phenomenology, University of Durham, South Road, Durham DH1 3LE, England, UK*

Received 14 February 2005; accepted 3 March 2005

Editor: P.V. Landshoff

Abstract

Antenna functions describe the infrared singular behaviour of colour-ordered QCD matrix elements due to the emission of unresolved partons inside an antenna formed by two hard partons. In this Letter, we show that antenna functions for hard gluon–gluon pairs can be systematically derived from the effective Lagrangian describing Higgs boson decay into gluons, and compute the infrared structure of the colour-ordered Higgs boson decay matrix elements at NLO and NNLO.

© 2005 Elsevier B.V. Open access under [CC BY license](https://creativecommons.org/licenses/by/4.0/).

1. Introduction

Perturbative QCD corrections to exclusive jet observables are at present restricted to the next-to-leading order in perturbation theory, which is often insufficient to match the experimental precision on jet production reactions [1]. In the recent past, much progress was made to extend these calculations to the next-to-next-to-leading order (NNLO) in perturbation theory [2–14] and first results for exclusive NNLO cross sections became available recently [15–17].

The calculation of NNLO corrections to jet observables requires a method for the extraction of real radiation singularities arising from the emission of up to two unresolved (soft or collinear) partons in the final state. Several methods have been proposed recently [11] to accomplish the task of constructing so-called NNLO subtraction terms.

In [14], we described the derivation of NNLO subtraction terms for $e^+e^- \rightarrow 2j$ based on full four-parton tree-level and three-parton one-loop matrix elements, which can be integrated analytically over the appropriate

E-mail addresses: gehra@phys.ethz.ch (A. Gehrmann-De Ridder), gehr@physik.unizh.ch (T. Gehrmann), e.w.n.glover@durham.ac.uk (E.W.N. Glover).

phase spaces [13]. These NNLO subtraction terms were used subsequently [17] in the calculation of the NNLO corrections to one of the colour factors contributing to $e^+e^- \rightarrow 3j$.

Subtraction terms derived from full matrix elements can be viewed as antenna functions, encapsulating all singular limits due to unresolved partonic emission between two colour-connected hard partons [6,18]. In particular, process-independent antenna functions describing arbitrary QCD multiparticle processes can be directly related to three-parton matrix elements at NLO (one unresolved parton radiating between two colour-connected hard partons) and four-parton matrix elements at NNLO (two unresolved partons radiating between two colour-connected hard partons).

QCD calculations of jet observables require three different types of antenna functions, corresponding to the different pairs of hard partons forming the antenna: quark–antiquark, quark–gluon and gluon–gluon antenna functions. The quark–antiquark antenna functions can be obtained from the $e^+e^- \rightarrow 2j$ real radiation corrections at NLO and NNLO [14]. In [19], we described how the quark–gluon antenna functions could be derived from the purely QCD (i.e., non-supersymmetric) NLO and NNLO corrections to the decay of a heavy neutralino into a massless gluino plus partons. It is the purpose of this Letter to complete the derivation of NLO and NNLO antenna functions by considering the corrections to the decay of a Higgs boson into gluons as template for the gluon–gluon antenna functions.

The Higgs boson coupling to gluons is mediated through massive quark loops, which decouple for large quark masses, thus yielding an effective theory containing the interaction of the Higgs field with the gluonic field strength tensor [20]. In this effective theory, the Higgs boson decay rate [21] and inclusive Higgs boson production cross sections [22–24] were computed to NNLO. Most recently, NNLO results for the exclusive Higgs boson production cross section [16] were obtained as well.

In the following, we will show which individual real radiation processes contribute to the Higgs boson decay in the effective theory at NLO and NNLO, and that the real radiation singularities arising at these orders precisely match the infrared singularity structure obtained from an infrared factorization formula [25], such that these Higgs boson decay matrix elements can be used to derive the gluon–gluon antenna functions at NNLO.

2. Effective Lagrangian and Feynman rules

At tree level, the Higgs boson does not couple either to the gluon or to massless quarks. In higher orders in perturbation theory, heavy quark loops introduce a coupling between the Higgs boson and gluons. In the limit of infinitely massive quarks, these loops give rise to an effective Lagrangian [20] mediating the coupling between the scalar Higgs field and the gluon field strength tensor:

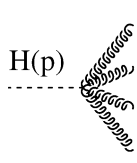
$$\mathcal{L}_{\text{int}} = -\frac{\lambda}{4} H F_a^{\mu\nu} F_{a,\mu\nu}. \quad (2.1)$$

The coupling λ has inverse mass dimension. It can be computed by matching [21,26] the effective theory to the full standard model cross sections [27].

The Feynman rules following from this Lagrangian are:

$$\begin{array}{c} \text{H}(p) \\ \text{-----} \\ \text{g}^a(k_0, \varepsilon_{0,\mu}) \\ \text{g}^b(k_1, \varepsilon_{1,\nu}) \end{array} = i\lambda\delta^{ab}(g^{\mu\nu}k_0 \cdot k_1 - k_0^\nu k_1^\mu), \quad (2.2)$$

$$\begin{array}{c} \text{H}(p) \\ \text{-----} \\ \text{g}^a(k_0, \varepsilon_{0,\mu}) \\ \text{g}^b(k_1, \varepsilon_{1,\nu}) \\ \text{g}^c(k_2, \varepsilon_{2,\rho}) \end{array} = -g_s\lambda f^{abc}(g^{\mu\nu}(k_0^\rho - k_1^\rho) + g^{\nu\rho}(k_1^\mu - k_2^\mu) + g^{\rho\mu}(k_2^\nu - k_0^\nu)), \quad (2.3)$$



$$\begin{aligned}
H(p) \begin{matrix} g^a(k_0, \epsilon_{0,\mu}) \\ g^b(k_1, \epsilon_{1,\nu}) \\ g^c(k_2, \epsilon_{2,\rho}) \\ g^d(k_3, \epsilon_{3,\sigma}) \end{matrix} &= -i g_s^2 \lambda [f^{abe} f^{cde} (g^{\mu\rho} g^{\nu\sigma} - g^{\mu\sigma} g^{\nu\rho}) \\
&+ f^{ade} f^{bce} (g^{\mu\nu} g^{\rho\sigma} - g^{\mu\rho} g^{\nu\sigma}) + f^{ace} f^{dbe} (g^{\mu\sigma} g^{\nu\rho} - g^{\mu\nu} g^{\rho\sigma})]. \quad (2.4)
\end{aligned}$$

The momenta are always incoming.

In the present context, the value of λ is irrelevant, but we do have to take into account that λ is renormalized in the effective theory. The renormalization constant of λ was computed to all orders in [28]; it reads

$$Z_\lambda = \frac{1}{1 - \beta(\alpha_s)/\epsilon} = 1 - \frac{\alpha_s}{2\pi} \frac{\beta_0}{\epsilon} + \left(\frac{\alpha_s}{2\pi}\right)^2 \left[\frac{\beta_0^2}{\epsilon^2} - \frac{\beta_1}{\epsilon} \right] + \mathcal{O}(\alpha_s^3) \quad (2.5)$$

with

$$\beta_0 = \frac{11N - 2N_F}{6}, \quad \beta_1 = \frac{34N^3 - 13N^2 N_F + 3N_F}{12N}. \quad (2.6)$$

3. Colour-ordered amplitudes in Higgs boson decay

The basic process for the decay of a Higgs boson into partons is $H(q) \rightarrow g(p_1)g(p_2)$. Its amplitude reads

$$\mathcal{M}_{g_1 g_2}^0 = i\lambda \delta^{a_1 a_2} M_{gg}^0(p_1, p_2). \quad (3.1)$$

The amplitude contains two colour connected (hard) partons which form two antennae, since unresolved parton emission can take place on both fundamental colour lines connecting the gluons p_1 and p_2 , as illustrated in Fig. 1.

The squared matrix element, averaged over identical gluons in the final state is

$$\mathcal{T}_{gg}^0(q^2) \equiv \frac{1}{2} |\mathcal{M}_{g_1 g_2}^0|^2 = \frac{1}{2} \lambda^2 (N^2 - 1) |M_{gg}^0(p_1, p_2)|^2 = \frac{1}{4} (N^2 - 1) \lambda^2 (1 - \epsilon) (q^2)^2. \quad (3.2)$$

$\mathcal{T}_{gg}^0(q^2)$ serves as normalization for antenna functions obtained from higher order corrections to this matrix element.

To demonstrate the cancellation of infrared divergences at NLO, we compute the renormalized one-loop QCD correction to the $H(q) \rightarrow g(p_1)g(p_2)$ decay,

$$\begin{aligned}
\mathcal{T}_{gg}^1(q^2) &\equiv \frac{1}{2} 2 \text{Re} |\mathcal{M}_{g_1 g_2}^0 \mathcal{M}_{g_1 g_2}^{1,*}| \\
&= \left(\frac{\alpha_s}{2\pi}\right) 2(q^2)^{-\epsilon} \mathcal{T}_{gg}^0(q^2) \left\{ N \left[-\frac{1}{\epsilon^2} - \frac{11}{6\epsilon} + \frac{7\pi^2}{12} + \left(-1 + \frac{7}{3}\zeta_3\right)\epsilon + \left(-3 - \frac{73\pi^4}{1440}\right)\epsilon^2 \right] \right. \\
&\quad \left. + \frac{N_F}{3\epsilon} + \mathcal{O}(\epsilon^3) \right\}. \quad (3.3)
\end{aligned}$$

The infrared poles of this one-loop correction can be expressed in terms of the infrared singularity operator [25]

$$I_{gg}^{(1)}(\epsilon, q^2) = -\frac{e^{\epsilon\gamma}}{2\Gamma(1-\epsilon)} \left[N \left(\frac{1}{\epsilon^2} + \frac{\beta_0}{N\epsilon} \right) (-q^2)^{-\epsilon} \right], \quad (3.4)$$

as

$$\text{Poles}(\mathcal{T}_{gg}^1(q^2)) = \left(\frac{\alpha_s}{2\pi}\right) 4 \text{Re} I_{gg}^{(1)}(\epsilon, q^2) \mathcal{T}_{gg}^0(q^2). \quad (3.5)$$

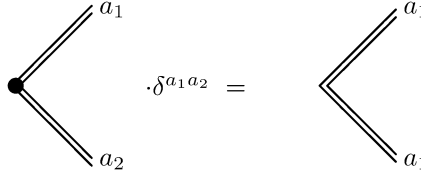


Fig. 1. Colour flow contained in tree level decay $H \rightarrow gg$. Double (single) lines denote adjoint (fundamental) colour indices.

This expression has to be compared to the $2 \operatorname{Re} \mathbf{I}_{q\bar{q}}^{(1)}(\epsilon, q^2)$, which is obtained in the decay of a virtual photon into a quark–antiquark pair $\gamma^* \rightarrow q\bar{q}$ at one loop [14] and the factor $4 \operatorname{Re} \mathbf{I}_{qg}^{(1)}(\epsilon, q^2)$, which is obtained in the decay of a neutralino into a gluino–gluon pair $\tilde{\chi} \rightarrow \tilde{g}g$ at one loop [19]. The factor 4 in (3.5) appears since the leading order process $H \rightarrow gg$ contains two distinct gluon–gluon antennae, just as $\tilde{\chi} \rightarrow \tilde{g}g$ contains two quark–gluon antennae, but in contrast to the single quark–antiquark antenna in $\gamma^* \rightarrow q\bar{q}$.

4. NLO antenna functions

Two different emissions off a gluon–gluon pair appear at NLO: either the emission of an additional gluon or the splitting of one gluon into a quark–antiquark pair. In the context of Higgs boson decay, these correspond to the tree level processes $H \rightarrow ggg$ and $H \rightarrow gq\bar{q}$.

The tree level amplitude for $H(q) \rightarrow g(p_1)g(p_2)g(p_3)$ contains only a single colour structure, $f^{a_1 a_2 a_3}$:

$$\mathcal{M}_{g_1 g_2 g_3}^0 = i\lambda g f^{a_1 a_2 a_3} M_{ggg}^0(p_1, p_2, p_3). \quad (4.1)$$

Squaring the matrix element and dividing by a symmetry factor to account for identical gluons in the final state yields

$$\frac{1}{3!} |\mathcal{M}_{g_1 g_2 g_3}^0|^2 = \lambda^2 g^2 (N^2 - 1) N \frac{1}{3!} |M_{ggg}^0(p_1, p_2, p_3)|^2 \quad (4.2)$$

with

$$\begin{aligned} \frac{1}{3!} |M_{ggg}^0(p_1, p_2, p_3)|^2 &= \frac{1}{2} (1 - \epsilon) \frac{1}{3} \left(\frac{2s_{12}^2 s_{13}}{s_{13} s_{23}} + \frac{2s_{12}^2 s_{13}}{s_{12} s_{23}} + \frac{2s_{12}^2 s_{23}}{s_{12} s_{13}} \right. \\ &\quad \left. + \frac{2s_{12} s_{13}}{s_{23}} + \frac{2s_{12} s_{23}}{s_{13}} + \frac{2s_{13} s_{23}}{s_{12}} + 12s_{123} \right) - \frac{2}{3} s_{123}. \end{aligned} \quad (4.3)$$

The factor $1/3$ in the above equation reflects the fact that the $H \rightarrow ggg$ matrix element contains three different antenna configurations (corresponding to the three different possibilities of identifying the two hard gluons and the one unresolved gluon). The effect of the symmetrization over the three gluons is that these three antenna configurations are averaged over. To illustrate the antenna factorization, the leading order matrix element (without the symmetrization factor for two identical gluons) is factored out.

The behaviour of this matrix element in the kinematical limits where one parton becomes unresolved is as follows:

(1) Collinear limits:

$$\frac{1}{3!} |\mathcal{M}_{g_i g_j g_k}^0|^2 \xrightarrow{g_i \parallel g_j} (4\pi\alpha_s) 2 \frac{\mathcal{T}_{gg}^0(s_{ijk})}{3} \frac{1}{s_{ij}} N P_{g \rightarrow gg}(z) \quad (4.4)$$

with z being the momentum fraction of one of the collinear partons and the splitting function

$$P_{g \rightarrow gg}(z) = 2 \left[\frac{z}{1-z} + \frac{1-z}{z} + z(1-z) \right].$$

(2) Soft limits:

$$\frac{1}{3!} |\mathcal{M}_{g_i g_j g_k}^0|^2 \xrightarrow{g_j \rightarrow 0} (4\pi\alpha_s) 2 \frac{\mathcal{T}_{gg}^0(s_{ijk})}{3} N \frac{2s_{ik}}{s_{ij}s_{jk}}. \quad (4.5)$$

Besides the symmetry factor $1/3$ accounting for the average over the three different antenna configurations, we observe an overall factor 2, corresponding to the presence of two distinct antenna functions in the basic two-parton matrix element, Fig. 1.

To obtain antenna functions describing the emission of an unresolved gluon j off an antenna containing two hard gluons i, k , the matrix element (4.3) has to be split into three individual antenna configurations. Each individual antenna configuration contains only one soft limit. Each collinear $g \rightarrow gg$ is split between the two antenna configurations appropriate to the two final state gluons involved in the splitting, as discussed in [6,18].

Integration over the dipole phase space [13] yields

$$\begin{aligned} \mathcal{T}_{ggg}^1(q^2) &\equiv \int d\Phi_{D,ggg} \frac{1}{3!} |\mathcal{M}_{g_1 g_2 g_3}^0|^2 \\ &= \left(\frac{\alpha_s}{2\pi} \right) N \mathcal{T}_{gg}^0(q^2) (q^2)^{-\epsilon} \left[\frac{2}{\epsilon^2} + \frac{11}{3\epsilon} + \frac{73}{6} - \frac{7\pi^2}{6} + \left(\frac{451}{12} - \frac{77\pi^2}{36} - \frac{50}{3} \zeta_3 \right) \epsilon \right. \\ &\quad \left. + \left(\frac{2729}{24} - \frac{511\pi^2}{72} - \frac{275}{9} \zeta_3 - \frac{71\pi^4}{720} \right) \epsilon^2 + \mathcal{O}(\epsilon^3) \right]. \end{aligned} \quad (4.6)$$

The tree level amplitude for $H(q) \rightarrow g(p_1)q(p_3)\bar{q}(p_4)$ contains only a single colour structure $T_{i_3 i_4}^{a_1}$:

$$\mathcal{M}_{g_1 q_3 \bar{q}_4}^0 = i\lambda g T_{i_3 i_4}^{a_1} M_{gq\bar{q}}^0(p_1, p_3, p_4), \quad (4.7)$$

yielding

$$|\mathcal{M}_{g_1 q_3 \bar{q}_4}^0|^2 = \lambda^2 g^2 \frac{N^2 - 1}{2} |M_{gq\bar{q}}^0(p_1, p_3, p_4)|^2 \quad (4.8)$$

with

$$|M_{gq\bar{q}}^0(p_1, p_3, p_4)|^2 = \frac{1}{2} (1 - \epsilon) \left(2 \frac{(s_{13} + s_{14})^2}{s_{34}} \right) - 2 \frac{s_{13}s_{14}}{s_{34}}. \quad (4.9)$$

The only singular configuration contained in this matrix element is the collinear quark–antiquark limit, which is as follows:

$$|\mathcal{M}_{g_1 q_3 \bar{q}_4}^0|^2 \xrightarrow{q_3 \parallel \bar{q}_4} 2(4\pi\alpha_s) \mathcal{T}_{gg}^0(s_{134}) \frac{1}{s_{34}} P_{g \rightarrow q\bar{q}}(z) \quad (4.10)$$

with the collinear splitting function

$$P_{g \rightarrow q\bar{q}}(z) = 1 - \frac{2z(1-z)}{1-\epsilon}.$$

The factor 2 arises from the fact that two gluon–gluon antennae are contained in the matrix element (3.1) as above.

Integration over the dipole phase space [13] and summing over final state quark flavours yields

$$\begin{aligned} \mathcal{T}_{gq\bar{q}}^1(q^2) &\equiv \int d\Phi_{D,gq\bar{q}} \sum_q |\mathcal{M}_{g_1q_3\bar{q}_4}^0|^2 \\ &= \left(\frac{\alpha_s}{2\pi}\right) N_F \mathcal{T}_{gg}^0(q^2) (q^2)^{-\epsilon} \left[-\frac{2}{3\epsilon} - \frac{7}{3} + \left(-\frac{15}{2} + \frac{7\pi^2}{18}\right)\epsilon \right. \\ &\quad \left. + \left(-\frac{93}{4} + \frac{49\pi^2}{36} + \frac{50}{9}\zeta_3\right)\epsilon^2 + \mathcal{O}(\epsilon^3) \right]. \end{aligned} \quad (4.11)$$

Summing over both three parton final states, we find

$$\mathcal{Poles}(\mathcal{T}_{ggg}^1(q^2) + \mathcal{T}_{gq\bar{q}}^1(q^2)) = -\left(\frac{\alpha_s}{2\pi}\right) 4 \operatorname{Re} \mathbf{I}_{gg}^{(1)}(\epsilon, q^2) \mathcal{T}_{gg}^0(q^2), \quad (4.12)$$

such that the NLO corrected Higgs boson decay rate into partons is finite:

$$\mathcal{Poles}(\mathcal{T}_{gg}^1(q^2)) + \mathcal{Poles}(\mathcal{T}_{ggg}^1(q^2) + \mathcal{T}_{gq\bar{q}}^1(q^2)) = 0. \quad (4.13)$$

We recover the finite NLO contribution to the Higgs boson decay rate into partons in the effective theory as

$$\mathcal{F}inite(\mathcal{T}_{gg}^1(q^2)) + \mathcal{F}inite(\mathcal{T}_{ggg}^1(q^2) + \mathcal{T}_{gq\bar{q}}^1(q^2)) = \frac{\alpha_s}{2\pi} \left(\frac{73}{6}N - \frac{7}{3}N_F\right) \mathcal{T}_{gg}^0(q^2), \quad (4.14)$$

which is in agreement with [21].

5. Structure of NNLO antenna functions

In the NNLO calculation of jet observables, two different types of antenna functions are required: (a) the one-loop correction to the three-parton antenna functions which appeared at NLO in tree-level form, and (b) the tree-level four-parton antenna functions. In this section, we present all Higgs boson decay matrix elements needed for the derivation of these antenna functions, and demonstrate that these matrix elements contain the same infrared singularities as processes involving final state emission off a gluon–gluon antenna.

The renormalized one-loop corrections to the three-parton antenna functions have the same colour structure as their tree level counterparts listed above. To expose the infrared structure of the resulting one-loop matrix elements, they are integrated over the corresponding dipole phase space [13], yielding

$$\begin{aligned} \mathcal{T}_{ggg}^2(q^2) &\equiv \int d\Phi_{D,ggg} \frac{1}{6} 2 \operatorname{Re}(\mathcal{M}_{g_1g_2g_3}^0 \mathcal{M}_{g_1g_2g_3}^{1,*}) \\ &= \left(\frac{\alpha_s}{2\pi}\right)^2 \mathcal{T}_{gg}^0(q^2) (q^2)^{-2\epsilon} \left[N^2 \left(-\frac{9}{2\epsilon^4} - \frac{121}{6\epsilon^3} + \frac{1}{\epsilon^2} \left(-\frac{170}{3} + \frac{71\pi^2}{12} \right) \right. \right. \\ &\quad \left. \left. + \frac{1}{\epsilon} \left(-\frac{23195}{108} + \frac{341\pi^2}{18} + 72\zeta_3 \right) + \left(-\frac{173249}{216} + \frac{13831\pi^2}{216} + \frac{2266}{9}\zeta_3 - \frac{995\pi^4}{720} \right) \right) \right. \\ &\quad \left. + NN_F \left(\frac{2}{\epsilon^3} + \frac{11}{3\epsilon^2} + \frac{1}{\epsilon} \left(\frac{37}{3} - \frac{7\pi^2}{6} \right) + \left(\frac{467}{12} - \frac{77\pi^2}{36} - \frac{50}{3}\zeta_3 \right) \right) + \mathcal{O}(\epsilon) \right], \end{aligned} \quad (5.1)$$

$$\begin{aligned} \mathcal{T}_{gq\bar{q}}^2(q^2) &\equiv \int d\Phi_{D,gq\bar{q}} 2 \operatorname{Re}(\mathcal{M}_{g_1q_3\bar{q}_4}^0 \mathcal{M}_{g_1q_3\bar{q}_4}^{1,*}) \\ &= \left(\frac{\alpha_s}{2\pi}\right)^2 \mathcal{T}_{gg}^0(q^2) (q^2)^{-2\epsilon} \left[NN_F \left(\frac{4}{3\epsilon^3} + \frac{25}{3\epsilon^2} + \frac{1}{\epsilon} \left(\frac{805}{27} - \frac{16\pi^2}{9} \right) \right) \right. \end{aligned}$$

$$\begin{aligned}
& + \left(\frac{2926}{27} - \frac{947\pi^2}{108} - \frac{188}{9}\zeta_3 \right) \\
& + \frac{N_F}{N} \left(-\frac{1}{3\epsilon^3} - \frac{41}{18\epsilon^2} + \frac{1}{\epsilon} \left(-\frac{325}{27} + \frac{\pi^2}{2} \right) + \left(-\frac{18457}{324} + \frac{41\pi^2}{12} + \frac{74}{9}\zeta_3 \right) \right) \\
& + N_F^2 \left(-\frac{4}{9\epsilon^2} - \frac{7}{9\epsilon} + \left(\frac{85}{162} + \frac{\pi^2}{18} \right) \right) + \mathcal{O}(\epsilon). \tag{5.2}
\end{aligned}$$

Three different four-parton final states appear in the gluon–gluon antenna functions at NNLO: $gggg$, $q\bar{q}gg$ and $q\bar{q}q'\bar{q}'$. In contrast to the tree level three-parton Higgs boson decay matrix elements, which contained only one non-trivial colour ordering each, these four-parton matrix elements all contain several colour-orderings.

The amplitude for $H(q) \rightarrow g(p_1)g(p_2)g(p_3)g(p_4)$ can then be expressed as sum over the permutations of the gluon colour indices:

$$\mathcal{M}_{g_1g_2g_3g_4}^0 = i\lambda g^4 \sum_{(i,j,k) \in P(2,3,4)} \text{Tr}(T^{a_1}T^{a_i}T^{a_j}T^{a_k}) M_{gggg}^0(p_1, p_i, p_j, p_k), \tag{5.3}$$

where the sum runs over all six permutations of three of the gluon colour indices, thus excluding any configurations which can be related by cyclic permutations of all four colour indices. Its colour flow is illustrated in Fig. 2.

The resulting squared matrix element, averaged over identical final state gluon permutations is

$$\frac{1}{4!} |\mathcal{M}_{g_1g_2g_3g_4}^0|^2 = \lambda^2 g^4 \frac{N^2 - 1}{16} \frac{1}{4!} N^2 \sum_{(i,j,k) \in P(2,3,4)} |M_{gggg}^0(p_1, p_i, p_j, p_k)|^2. \tag{5.4}$$

It should be noted that this squared matrix element contains only the leading colour term obtained from the squares of the individual colour-ordered amplitudes, as expected in the colour ordered formulation for a process with four gluons [29,30].

The tree level amplitude for $H(q) \rightarrow g(p_1)g(p_2)q(p_3)\bar{q}(p_4)$ contains two colour structures, depicted in Fig. 3

$$\mathcal{M}_{g_1g_2q_3\bar{q}_4}^0 = i\lambda g^2 \left[(T^{a_1}T^{a_2})_{i_3i_4} M_{ggq\bar{q}}^0(p_1, p_2, p_3, p_4) + (T^{a_2}T^{a_1})_{i_3i_4} M_{ggq\bar{q}}^0(p_2, p_1, p_3, p_4) \right]. \tag{5.5}$$

The squared matrix element, averaged over identical gluons in the final state and summed over quark flavours, reads

$$\begin{aligned}
\frac{1}{2} |\mathcal{M}_{g_1g_2q_3\bar{q}_4}^0|^2 & = \lambda^2 g^4 \frac{N^2 - 1}{8} N_F \left\{ N \left[|M_{ggq\bar{q}}^0(p_1, p_2, p_3, p_4)|^2 + |M_{ggq\bar{q}}^0(p_2, p_1, p_3, p_4)|^2 \right] \right. \\
& \left. - \frac{1}{N} |M_{ggq\bar{q}}^0(p_1, p_2, p_3, p_4) + M_{ggq\bar{q}}^0(p_2, p_1, p_3, p_4)|^2 \right\}. \tag{5.6}
\end{aligned}$$

Finally, the tree level amplitude for $H(q) \rightarrow q(p_1)q(p_2)q'(p_3)\bar{q}'(p_4)$ contains only a single colour structure, but can contain two flavour structures in the case of identical quark flavours $q = q'$:

$$\mathcal{M}_{q_1q_2q'_3\bar{q}'_4}^0 = i\lambda g^2 \left[T_{i_1i_2}^{a_1} T_{i_3i_4}^{a_1} M_{q\bar{q}q'\bar{q}'}^0(p_1, p_2, p_3, p_4) - \delta_{qq'} T_{i_1i_4}^{a_1} T_{i_3i_2}^{a_1} M_{q\bar{q}q'\bar{q}'}^0(p_1, p_4, p_3, p_2) \right]. \tag{5.7}$$

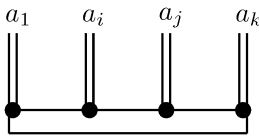


Fig. 2. Colour flow contained in the colour ordered amplitude $M_{gggg}^0(p_1, p_i, p_j, p_k)$ contributing to the tree level decay $H \rightarrow gggg$.

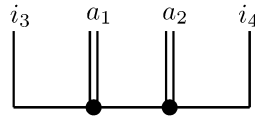


Fig. 3. Colour flow contained in the colour ordered amplitude $M_{ggq\bar{q}}^0(p_1, p_2, p_3, p_4)$ contributing to the tree level decay $H \rightarrow ggq\bar{q}$.

The squared matrix element, summed over quark flavours and averaged over identical configurations becomes

$$\begin{aligned} \frac{1}{2} \sum_F |\mathcal{M}_{q_1 q_2 q_3 \bar{q}_4}^0|^2 &= \lambda^2 g^4 \frac{N^2 - 1}{8} \left\{ N_F^2 |M_{q\bar{q}q'\bar{q}'}^0(p_1, p_2, p_3, p_4)|^2 \right. \\ &\quad \left. - \frac{N_F}{N} \delta_{qq'} \operatorname{Re}(M_{q\bar{q}q'\bar{q}'}^0(p_1, p_2, p_3, p_4) M_{q\bar{q}q'\bar{q}'}^{0,*}(p_1, p_4, p_3, p_2)) \right\}. \end{aligned} \quad (5.8)$$

The four-parton tree-level Higgs boson decay matrix elements can be integrated over the tripole phase space [13], thus making their infrared singularity structure explicit,

$$\begin{aligned} \mathcal{T}_{gggg}^2(q^2) &\equiv \int d\Phi_{T,gggg} \frac{1}{4!} |\mathcal{M}_{g_1 g_2 g_3 g_4}^0|^2 \\ &= \left(\frac{\alpha_s}{2\pi} \right)^2 \mathcal{T}_{gg}^0(q^2) (q^2)^{-2\epsilon} N^2 \left[\frac{5}{2\epsilon^4} + \frac{121}{12\epsilon^3} + \frac{1}{\epsilon^2} \left(\frac{436}{9} - \frac{11\pi^2}{3} \right) \right. \\ &\quad \left. + \frac{1}{\epsilon} \left(\frac{23455}{108} - \frac{1067\pi^2}{72} - \frac{379}{6} \zeta_3 \right) + \left(\frac{304951}{324} - \frac{7781\pi^2}{108} - \frac{2288}{9} \zeta_3 + \frac{479\pi^4}{720} \right) + \mathcal{O}(\epsilon) \right], \end{aligned} \quad (5.9)$$

$$\begin{aligned} \mathcal{T}_{ggq\bar{q}}^2(q^2) &\equiv \int d\Phi_{T,ggq\bar{q}} \frac{1}{2} |\mathcal{M}_{g_1 g_2 q_3 \bar{q}_4}^0|^2 \\ &= \left(\frac{\alpha_s}{2\pi} \right)^2 \mathcal{T}_{gg}^0(q^2) (q^2)^{-2\epsilon} \left[NN_F \left(-\frac{3}{2\epsilon^3} - \frac{155}{18\epsilon^2} + \frac{1}{\epsilon} \left(-\frac{523}{12} + \frac{79\pi^2}{36} \right) \right. \right. \\ &\quad \left. \left. + \left(-\frac{16579}{81} + \frac{1385\pi^2}{108} + 37\zeta_3 \right) \right) \right. \\ &\quad \left. + \frac{N_F}{N} \left(\frac{1}{3\epsilon^3} + \frac{41}{18\epsilon^2} + \frac{1}{\epsilon} \left(\frac{1327}{108} - \frac{\pi^2}{2} \right) + \left(\frac{4864}{81} - \frac{41\pi^2}{12} - \frac{86}{9} \zeta_3 \right) \right) + \mathcal{O}(\epsilon) \right], \end{aligned} \quad (5.10)$$

$$\begin{aligned} \mathcal{T}_{q\bar{q}q'\bar{q}'}^2(q^2) &\equiv \int d\Phi_{T,q\bar{q}q'\bar{q}'} \frac{1}{2} |\mathcal{M}_{q_1 \bar{q}_2 q_3 \bar{q}_4}^0|^2 \\ &= \left(\frac{\alpha_s}{2\pi} \right)^2 \mathcal{T}_{gg}^0(q^2) (q^2)^{-2\epsilon} \left[N_F^2 \left(\frac{1}{9\epsilon^2} + \frac{7}{9\epsilon} + \left(\frac{677}{162} - \frac{\pi^2}{6} \right) \right) + \frac{N_F}{N} \left(-\frac{5}{12} + \frac{\zeta_3}{3} \right) + \mathcal{O}(\epsilon) \right]. \end{aligned} \quad (5.11)$$

The sum of all NNLO subtraction terms yields the following infrared pole structure, which can be expressed in terms of NNLO infrared singularity operators [25],

$$\begin{aligned} \mathcal{Poles}(\mathcal{T}_{ggg}^2(q^2) + \mathcal{T}_{gq\bar{q}}^2(q^2) + \mathcal{T}_{gggg}^2(q^2) + \mathcal{T}_{ggq\bar{q}}^2(q^2) + \mathcal{T}_{q\bar{q}q'\bar{q}'}^2(q^2)) \\ &= \left(\frac{\alpha_s}{2\pi} \right)^2 \mathcal{T}_{gg}^0(q^2) (q^2)^{-2\epsilon} \left[N^2 \left(-\frac{2}{\epsilon^4} - \frac{121}{12\epsilon^3} + \frac{1}{\epsilon^2} \left(-\frac{74}{9} + \frac{9\pi^2}{4} \right) + \frac{1}{\epsilon} \left(\frac{65}{27} + \frac{33\pi^2}{8} + \frac{53}{6} \zeta_3 \right) \right) \right. \\ &\quad \left. + NN_F \left(\frac{11}{6\epsilon^3} + \frac{61}{18\epsilon^2} + \frac{1}{\epsilon} \left(-\frac{155}{108} - \frac{3\pi^2}{4} \right) \right) + \frac{N_F}{N} \left(\frac{1}{4\epsilon} \right) + N_F^2 \left(-\frac{1}{3\epsilon^2} \right) + \mathcal{O}(\epsilon^0) \right] \\ &= - \left(\frac{\alpha_s}{2\pi} \right)^2 \operatorname{Re} \left[-2\mathbf{I}_{gg}^{(1)}(\epsilon, q^2) (2\mathbf{I}_{gg}^{(1)}(\epsilon, q^2) + 2\mathbf{I}_{gg}^{(1),*}(\epsilon, q^2)) \mathcal{T}_{gg}^0(q^2) - 2\frac{\beta_0}{\epsilon} 2\mathbf{I}_{gg}^{(1)}(\epsilon, q^2) \mathcal{T}_{gg}^0(q^2) \right. \\ &\quad \left. + 4\mathbf{I}_{gg}^{(1)}(\epsilon, q^2) \mathcal{T}_{gg}^1(q^2) + 2e^{-\epsilon\gamma} \frac{\Gamma(1-2\epsilon)}{\Gamma(1-\epsilon)} \left(\frac{\beta_0}{\epsilon} + K \right) 2\mathbf{I}_{gg}^{(1)}(2\epsilon, q^2) \mathcal{T}_{gg}^0(q^2) + 2\mathbf{H}_{gg}^{(2)}(\epsilon, q^2) \mathcal{T}_{gg}^0(q^2) \right], \end{aligned} \quad (5.13)$$

where β_0 is the first term of the QCD β -function (2.6) and the constant K

$$K = \left(\frac{67}{18} - \frac{\pi^2}{6} \right) N - \frac{5}{9} N_F. \quad (5.14)$$

The final state dependent constant $\mathbf{H}_{gg}^{(2)}(\epsilon, q^2)$ contributes only at $\mathcal{O}(\epsilon^{-1})$:

$$\mathbf{H}_{gg}^{(2)}(\epsilon, q^2) = \frac{e^{\epsilon\gamma}}{4\epsilon\Gamma(1-\epsilon)} (2H_g^{(2)}) (-q^2)^{-2\epsilon} \quad (5.15)$$

with

$$H_g^{(2)} = \left(\frac{1}{2}\zeta_3 + \frac{5}{12} + \frac{11\pi^2}{144} \right) N^2 + \frac{5}{27} N_F^2 + \left(-\frac{\pi^2}{72} - \frac{89}{108} \right) N N_F - \frac{N_F}{4N}. \quad (5.16)$$

The above structure is to be compared with the renormalized purely virtual NNLO corrections (two-loop times tree plus one-loop self-interference), which were first computed by Harlander [31]:

$$\begin{aligned} \mathcal{T}_{gg}^2(q^2) &\equiv \frac{1}{2} [2 \operatorname{Re} |\mathcal{M}_{g_1 g_2}^0 \mathcal{M}_{g_1 g_2}^{2,*} | + |\mathcal{M}_{g_1 g_2}^1|^2] \\ &= \left(\frac{\alpha_s}{2\pi} \right)^2 (q^2)^{-2\epsilon} \mathcal{T}_{gg}^0(q^2) \left[N^2 \left(\frac{2}{\epsilon^4} + \frac{121}{12\epsilon^3} + \frac{1}{\epsilon^2} \left(\frac{74}{9} - \frac{9\pi^2}{4} \right) + \frac{1}{\epsilon} \left(-\frac{65}{27} - \frac{33\pi^2}{8} - \frac{53}{6}\zeta_3 \right) \right. \right. \\ &\quad \left. \left. + \left(\frac{11369}{324} + \frac{335\pi^2}{72} - \frac{451}{18}\zeta_3 + \frac{43\pi^4}{60} \right) \right) \right. \\ &\quad \left. + N N_F \left(-\frac{11}{6\epsilon^3} - \frac{61}{18\epsilon^2} + \frac{1}{\epsilon} \left(\frac{155}{108} + \frac{3\pi^2}{4} \right) + \left(-\frac{6337}{648} - \frac{25\pi^2}{36} + \frac{23}{9}\zeta_3 \right) \right) \right. \\ &\quad \left. + \frac{N_F}{N} \left(-\frac{1}{4\epsilon} + \left(\frac{67}{24} - 2\zeta_3 \right) \right) + N_F^2 \left(\frac{1}{3\epsilon^2} \right) + \mathcal{O}(\epsilon) \right]. \quad (5.17) \end{aligned}$$

It can be seen that the poles of the real radiation terms (5.12) cancel the poles of the purely virtual corrections:

$$\mathcal{Poles}(\mathcal{T}_{ggg}^2(q^2) + \mathcal{T}_{gq\bar{q}}^2(q^2) + \mathcal{T}_{gggg}^2(q^2) + \mathcal{T}_{ggq\bar{q}}^2(q^2) + \mathcal{T}_{q\bar{q}q'\bar{q}'}^2(q^2)) + \mathcal{Poles}(\mathcal{T}_{gg}^2(q^2)) = 0. \quad (5.18)$$

The infrared singularity structure (5.13) corresponds to the NNLO corrections to a tree level process containing two gluon–gluon antenna functions, as is the case for the Higgs boson decay.

An important check on our results is that the sum of all NNLO contributions

$$\begin{aligned} &\mathcal{F}inite(\mathcal{T}_{ggg}^2(q^2) + \mathcal{T}_{gq\bar{q}}^2(q^2) + \mathcal{T}_{gggg}^2(q^2) + \mathcal{T}_{ggq\bar{q}}^2(q^2) + \mathcal{T}_{q\bar{q}q'\bar{q}'}^2(q^2)) + \mathcal{F}inite(\mathcal{T}_{gg}^2(q^2)) \\ &= \left(\frac{\alpha_s}{2\pi} \right)^2 \left[N^2 \left(\frac{37631}{216} - \frac{121\pi^2}{36} - \frac{55}{2}\zeta_3 \right) + N N_F \left(-\frac{14509}{216} + \frac{11\pi^2}{9} + 2\zeta_3 \right) \right. \\ &\quad \left. + \frac{N_F}{N} \left(\frac{131}{24} - 3\zeta_3 \right) + N_F^2 \left(\frac{127}{27} - \frac{\pi^2}{9} \right) \right] \mathcal{T}_{gg}^0(q^2) \quad (5.19) \end{aligned}$$

agrees with the NNLO correction to the total Higgs boson decay rate into partons in the effective theory [21].

Eqs. (5.13) and (5.16) demonstrate that the NNLO three and four parton contributions to Higgs boson decay into massless partons display the same singularity structure as final state observables containing adjacent gluon–gluon pairs. It is therefore possible to derive colour-ordered gluon–gluon antenna functions from the Higgs boson decay matrix elements obtained here using the effective Lagrangian density (2.1).

6. Conclusions and outlook

QCD antenna functions describe the behaviour of QCD matrix elements in their infrared singular limits, corresponding to soft or collinear parton emission. They are constructed so that they describe all singular limits arising from emission of unresolved partons in between the two colour-connected hard partons that define the antenna. The quark–antiquark antenna functions are directly related to the physical matrix elements for $\gamma^* \rightarrow q\bar{q} + \text{partons}$. We demonstrated in a previous paper [19] that quark–gluon antenna functions could be obtained from an effective Lagrangian density describing neutralino decay into a gluino and other partons. Besides quark–antiquark and quark–gluon antenna functions, QCD calculations also require gluon–gluon antenna functions. In this Letter, we showed that gluon–gluon antenna functions can be obtained from physical Higgs boson decay matrix elements into partons, arising in an effective theory coupling the Higgs field to the gluonic field strength tensor.

We demonstrated that the physical Higgs boson decay matrix elements reproduce the singular structure of QCD gluon–gluon antenna functions at NLO and NNLO. We extracted the infrared structure for decay kinematics, as required for jet observables without partons in the initial state. By analytic continuation, the matrix elements derived here can also be continued to production (leading order process contains partons only in the initial state) or scattering (leading order process contains partons in initial and final state) kinematics, where they have to be integrated over the appropriate phase spaces. The phase space integrals for production kinematics were derived in [24], such that the antenna subtraction terms for this kinematical situation can in principle be derived.

With this and two preceding papers [14,19], we demonstrated that all QCD antenna functions can be derived (as opposed to constructed) from physical matrix elements: quark–antiquark antennae from the decay of a virtual photon into partons, quark–gluon antennae from neutralino decay into gluino plus partons and finally gluon–gluon antennae from Higgs boson decay into partons. The NNLO antenna subtraction functions obtained through this procedure will be reported in a subsequent publication [32].

Acknowledgements

This research was supported in part by the Swiss National Science Foundation (SNF) under contracts PMPD2-106101 and 200021-101874, by the UK Particle Physics and Astronomy Research Council and by the EU Fifth Framework Programme ‘Improving Human Potential’, Research Training Network ‘Particle Physics Phenomenology at High Energy Colliders’, contract HPRN-CT-2000-00149.

References

- [1] R.K. Ellis, W.J. Stirling, B.R. Webber, *QCD and Collider Physics*, Cambridge Univ. Press, Cambridge, 1996; G. Dissertori, I.G. Knowles, M. Schmelling, *Quantum Chromodynamics: High Energy Experiments and Theory*, Oxford Univ. Press, Oxford, 2003.
- [2] S. Moch, J.A.M. Vermaseren, A. Vogt, *Nucl. Phys. B* 688 (2004) 101, hep-ph/0403192; A. Vogt, S. Moch, J.A.M. Vermaseren, *Nucl. Phys. B* 691 (2004) 129, hep-ph/0404111.
- [3] Z. Bern, L.J. Dixon, A. Ghinculov, *Phys. Rev. D* 63 (2001) 053007, hep-ph/0010075; C. Anastasiou, E.W.N. Glover, C. Oleari, M.E. Tejeda-Yeomans, *Nucl. Phys. B* 601 (2001) 318, hep-ph/0010212; C. Anastasiou, E.W.N. Glover, C. Oleari, M.E. Tejeda-Yeomans, *Nucl. Phys. B* 601 (2001) 347, hep-ph/0011094; C. Anastasiou, E.W.N. Glover, C. Oleari, M.E. Tejeda-Yeomans, *Nucl. Phys. B* 605 (2001) 486, hep-ph/0101304; E.W.N. Glover, C. Oleari, M.E. Tejeda-Yeomans, *Nucl. Phys. B* 605 (2001) 467, hep-ph/0102201; C. Anastasiou, E.W.N. Glover, M.E. Tejeda-Yeomans, *Nucl. Phys. B* 629 (2002) 255, hep-ph/0201274; E.W.N. Glover, M.E. Tejeda-Yeomans, *JHEP* 0306 (2003) 033, hep-ph/0304169; E.W.N. Glover, *JHEP* 0404 (2004) 021, hep-ph/0401119; Z. Bern, A. De Freitas, L.J. Dixon, *JHEP* 0109 (2001) 037, hep-ph/0109078; Z. Bern, A. De Freitas, L.J. Dixon, *JHEP* 0203 (2002) 018, hep-ph/0201161;

- Z. Bern, A. De Freitas, L.J. Dixon, JHEP 0306 (2003) 028, hep-ph/0304168;
 Z. Bern, A. De Freitas, L.J. Dixon, A. Ghinculov, H.L. Wong, JHEP 0111 (2001) 031, hep-ph/0109079;
 T. Binoth, E.W.N. Glover, P. Marquard, J.J. van der Bij, JHEP 0205 (2002) 060, hep-ph/0202266;
 L.W. Garland, T. Gehrmann, E.W.N. Glover, A. Koukoutsakis, E. Remiddi, Nucl. Phys. B 627 (2002) 107, hep-ph/0112081;
 L.W. Garland, T. Gehrmann, E.W.N. Glover, A. Koukoutsakis, E. Remiddi, Nucl. Phys. B 642 (2002) 227, hep-ph/0206067;
 S. Moch, P. Uwer, S. Weinzierl, Phys. Rev. D 66 (2002) 114001, hep-ph/0207043;
 T. Gehrmann, E. Remiddi, Nucl. Phys. B 640 (2002) 379, hep-ph/0207020.
- [4] F.V. Tkachov, Phys. Lett. B 100 (1981) 65;
 K.G. Chetyrkin, F.V. Tkachov, Nucl. Phys. B 192 (1981) 159;
 V.A. Smirnov, Phys. Lett. B 460 (1999) 397, hep-ph/9905323;
 J.B. Tausk, Phys. Lett. B 469 (1999) 225, hep-ph/9909506;
 T. Binoth, G. Heinrich, Nucl. Phys. B 585 (2000) 741, hep-ph/0004013;
 S. Laporta, Int. J. Mod. Phys. A 15 (2000) 5087, hep-ph/0102033;
 T. Gehrmann, E. Remiddi, Nucl. Phys. B 580 (2000) 485, hep-ph/9912329;
 S. Moch, P. Uwer, S. Weinzierl, J. Math. Phys. 43 (2002) 3363, hep-ph/0110083;
 S. Weinzierl, Comput. Phys. Commun. 145 (2002) 357, math-ph/0201011;
 V.A. Smirnov, Evaluating Feynman Integrals, Springer Tracts of Modern Physics, Heidelberg, 2004.
- [5] L.J. Dixon, A. Signer, Phys. Rev. Lett. 78 (1997) 811, hep-ph/9609460;
 L.J. Dixon, A. Signer, Phys. Rev. D 56 (1997) 4031, hep-ph/9706285;
 Z. Nagy, Z. Trocsanyi, Phys. Rev. Lett. 79 (1997) 3604, hep-ph/9707309;
 S. Weinzierl, D.A. Kosower, Phys. Rev. D 60 (1999) 054028, hep-ph/9901277;
 W.B. Kilgore, W.T. Giele, Phys. Rev. D 55 (1997) 7183, hep-ph/9610433;
 Z. Nagy, Z. Trocsanyi, Phys. Rev. Lett. 87 (2001) 082001, hep-ph/0104315;
 Z. Nagy, Phys. Rev. Lett. 88 (2002) 122003, hep-ph/0110315;
 Z. Nagy, Phys. Rev. D 68 (2003) 094002, hep-ph/0307268;
 J. Campbell, R.K. Ellis, Phys. Rev. D 65 (2002) 113007, hep-ph/0202176.
- [6] J. Campbell, M.A. Cullen, E.W.N. Glover, Eur. Phys. J. C 9 (1999) 245, hep-ph/9809429.
- [7] Z. Bern, L.J. Dixon, D.C. Dunbar, D.A. Kosower, Nucl. Phys. B 425 (1994) 217, hep-ph/9403226;
 D.A. Kosower, Nucl. Phys. B 552 (1999) 319, hep-ph/9901201;
 D.A. Kosower, P. Uwer, Nucl. Phys. B 563 (1999) 477, hep-ph/9903515;
 Z. Bern, V. Del Duca, C.R. Schmidt, Phys. Lett. B 445 (1998) 168, hep-ph/9810409;
 Z. Bern, V. Del Duca, W.B. Kilgore, C.R. Schmidt, Phys. Rev. D 60 (1999) 116001, hep-ph/9903516;
 S. Catani, M. Grazzini, Nucl. Phys. B 591 (2000) 435, hep-ph/0007142;
 D.A. Kosower, Phys. Rev. Lett. 91 (2003) 061602, hep-ph/0301069;
 S. Weinzierl, JHEP 0307 (2003) 052, hep-ph/0306248.
- [8] Z. Bern, L.J. Dixon, D.A. Kosower, Phys. Rev. Lett. 70 (1993) 2677, hep-ph/9302280;
 Z. Kunszt, A. Signer, Z. Trocsanyi, Phys. Lett. B 336 (1994) 529, hep-ph/9405386;
 Z. Bern, L.J. Dixon, D.A. Kosower, Nucl. Phys. B 437 (1995) 259, hep-ph/9409393;
 E.W.N. Glover, D.J. Miller, Phys. Lett. B 396 (1997) 257, hep-ph/9609474;
 Z. Bern, L.J. Dixon, D.A. Kosower, S. Weinzierl, Nucl. Phys. B 489 (1997) 3, hep-ph/9610370;
 J.M. Campbell, E.W.N. Glover, D.J. Miller, Phys. Lett. B 409 (1997) 503, hep-ph/9706297;
 Z. Bern, L.J. Dixon, D.A. Kosower, Nucl. Phys. B 513 (1998) 3, hep-ph/9708239.
- [9] A. Gehrmann-De Ridder, E.W.N. Glover, Nucl. Phys. B 517 (1998) 269, hep-ph/9707224;
 J. Campbell, E.W.N. Glover, Nucl. Phys. B 527 (1998) 264, hep-ph/9710255.
- [10] S. Catani, M. Grazzini, Phys. Lett. B 446 (1999) 143, hep-ph/9810389;
 S. Catani, M. Grazzini, Nucl. Phys. B 570 (2000) 287, hep-ph/9908523;
 F.A. Berends, W.T. Giele, Nucl. Phys. B 313 (1989) 595;
 V. Del Duca, A. Frizzo, F. Maltoni, Nucl. Phys. B 568 (2000) 211, hep-ph/9909464.
- [11] D.A. Kosower, Phys. Rev. D 67 (2003) 116003, hep-ph/0212097;
 S. Weinzierl, JHEP 0303 (2003) 062, hep-ph/0302180;
 W.B. Kilgore, Phys. Rev. D 70 (2004) 031501, hep-ph/0403128;
 M. Grazzini, S. Frixione, hep-ph/0411399.
- [12] G. Heinrich, Nucl. Phys. B (Proc. Suppl.) 116 (2003) 368, hep-ph/0211144;
 C. Anastasiou, K. Melnikov, F. Petriello, Phys. Rev. D 69 (2004) 076010, hep-ph/0311311;
 T. Binoth, G. Heinrich, Nucl. Phys. B 693 (2004) 134, hep-ph/0402265;
 G. Heinrich, Nucl. Phys. B (Proc. Suppl.) 135 (2004) 290, hep-ph/0406332.
- [13] A. Gehrmann-De Ridder, T. Gehrmann, G. Heinrich, Nucl. Phys. B 682 (2004) 265, hep-ph/0311276.

- [14] A. Gehrmann-De Ridder, T. Gehrmann, E.W.N. Glover, Nucl. Phys. B 691 (2004) 195, hep-ph/0403057.
- [15] C. Anastasiou, K. Melnikov, F. Petriello, Phys. Rev. Lett. 93 (2004) 032002, hep-ph/0402280.
- [16] C. Anastasiou, K. Melnikov, F. Petriello, Phys. Rev. Lett. 93 (2004) 262002, hep-ph/0409088;
C. Anastasiou, K. Melnikov, F. Petriello, hep-ph/0501130.
- [17] A. Gehrmann-De Ridder, T. Gehrmann, E.W.N. Glover, Nucl. Phys. B (Proc. Suppl.) 135 (2004) 97, hep-ph/0407023.
- [18] D.A. Kosower, Phys. Rev. D 57 (1998) 5410, hep-ph/9710213.
- [19] A. Gehrmann-De Ridder, T. Gehrmann, E.W.N. Glover, Phys. Lett. B 612 (2005) 36, hep-ph/0501291.
- [20] F. Wilczek, Phys. Rev. Lett. 39 (1977) 1304;
M.A. Shifman, A.I. Vainshtein, V.I. Zakharov, Phys. Lett. B 78 (1978) 443;
J.R. Ellis, M.K. Gaillard, D.V. Nanopoulos, C.T. Sachrajda, Phys. Lett. B 83 (1979) 339;
T. Inami, T. Kubota, Y. Okada, Z. Phys. C 18 (1983) 69.
- [21] K.G. Chetyrkin, B.A. Kniehl, M. Steinhauser, Phys. Rev. Lett. 79 (1997) 353, hep-ph/9705240.
- [22] S. Catani, D. de Florian, M. Grazzini, JHEP 0105 (2001) 025, hep-ph/0102227;
S. Catani, D. de Florian, M. Grazzini, JHEP 0201 (2002) 015, hep-ph/0111164.
- [23] R.V. Harlander, W.B. Kilgore, Phys. Rev. D 64 (2001) 013015, hep-ph/0102241;
R.V. Harlander, W.B. Kilgore, Phys. Rev. Lett. 88 (2002) 201801, hep-ph/0201206;
R.V. Harlander, W.B. Kilgore, JHEP 0210 (2002) 017, hep-ph/0208096;
R.V. Harlander, W.B. Kilgore, Phys. Rev. D 68 (2003) 013001, hep-ph/0304035.
- [24] C. Anastasiou, K. Melnikov, Nucl. Phys. B 646 (2002) 220, hep-ph/0207004;
C. Anastasiou, K. Melnikov, Phys. Rev. D 67 (2003) 037501, hep-ph/0208115.
- [25] S. Catani, Phys. Lett. B 427 (1998) 161, hep-ph/9802439;
G. Sterman, M.E. Tejeda-Yeomans, Phys. Lett. B 552 (2003) 48, hep-ph/0210130.
- [26] B.A. Kniehl, M. Spira, Z. Phys. C 69 (1995) 77, hep-ph/9505225;
K.G. Chetyrkin, B.A. Kniehl, M. Steinhauser, Nucl. Phys. B 510 (1998) 61, hep-ph/9708255.
- [27] D. Graudenz, M. Spira, P.M. Zerwas, Phys. Rev. Lett. 70 (1993) 1372;
M. Spira, A. Djouadi, D. Graudenz, P.M. Zerwas, Nucl. Phys. B 453 (1995) 17, hep-ph/9504378;
A. Djouadi, M. Spira, P.M. Zerwas, Z. Phys. C 70 (1996) 427, hep-ph/9511344;
M. Spira, Fortschr. Phys. 46 (1998) 203, hep-ph/9705337.
- [28] V.P. Spiridonov, K.G. Chetyrkin, Sov. J. Nucl. Phys. 47 (1988) 522, Yad. Fiz. 47 (1988) 818 (in Russian).
- [29] F.A. Berends, W.T. Giele, Nucl. Phys. B 294 (1987) 700;
M. Mangano, S. Parke, Z. Xu, Nucl. Phys. B 298 (1988) 653;
M. Mangano, Nucl. Phys. B 309 (1988) 461;
L.J. Dixon, in: D. Soper (Ed.), Proceedings of Theoretical Advanced Study Institute in Elementary Particle Physics (TASI '95): QCD and Beyond, World Scientific, Singapore, 1996, p. 539, hep-ph/9601359.
- [30] V. Del Duca, L.J. Dixon, F. Maltoni, Nucl. Phys. B 571 (2000) 51, hep-ph/9910563;
F. Maltoni, K. Paul, T. Stelzer, S. Willenbrock, Phys. Rev. D 67 (2003) 014026, hep-ph/0209271.
- [31] R.V. Harlander, Phys. Lett. B 492 (2000) 74, hep-ph/0007289.
- [32] A. Gehrmann-De Ridder, T. Gehrmann, E.W.N. Glover, in preparation.